

Photovoltaic performance of dye-sensitized solar cells using TiO₂ nanotubes aggregates produced by hydrothermal synthesis

Qiufan Chen*, Xiaonan Sun^{*,‡}, Anping Liu*, Qifeng Zhang[†],
Guozhong Cao[†] and Xiaoyuan Zhou^{*,†,§}

^{*}*Department of Applied Physics, Chongqing University,
Chongqing 400044, P. R. China*

[†]*Department of Materials Science and Engineering,
University of Washington, Seattle, USA*

[‡]*23063907@qq.com*

[§]*xiaoyuan2013@cqu.edu.cn*

Received 10 March 2015

Accepted 4 May 2015

Published 16 September 2015

This paper reports the synthesis, detailed structural characterization of aggregated TiO₂ nanotubes and the application of such aggregated TiO₂ nanotubes as photoelectrodes in solar cells (dye sensitized DSCs). A maximum overall conversion efficiency of 7.9% has been achieved, which use conventional dyes without any additional chemical treatments under circumstances of an open-circuit voltage of 710 mV, a short-circuit current density of 16.8 mA/cm², and a fill factor of 66%. This impressive performance is believed to attribute to the micron-sized aggregate structure which may be favorable for light harvesting, the desired high specific surface area and pure anatase phase for dye absorption. This significant improvement in the conversion efficiency indicates that DSCs based on aggregated TiO₂ nanotubes are a promising alternative to semiconductor-based solar cells.

Keywords: Aggregated TiO₂ nanotubes; dye-sensitized solar cells; power conversion efficiency; hydrothermal synthesis.

PACS numbers: 61.46.Fg, 84.60.Jt

1. Introduction

With the emergence of nanotechnology and the fabrication of nanoscale oxides, dye sensitized solar cells (DSCs) based on hierarchically structured photoelectrodes have attracted wide attention because of the potential to significantly improve light absorption and photocurrent generation as well as to reduce the cost of photovoltaic devices.^{1–12} Hierarchically structured photoelectrodes are defined

[§]Corresponding author.

as a class of photoelectrodes that are made of films consisting of primary oxide nanostructures, for example, ZnO or TiO₂ nanocrystallites. However, these primary nanostructures form a secondary spherical or one-dimensional. When used in DSCs, the hierarchically structured photoelectrode films not only provide a high surface area for the adsorption of dye molecules, but also are able to offer extra functions to improve the solar cell performance, for example, generating light scattering, enhancing the transport of injected electrons, and/or facilitating the diffusion of the electrolyte. A noticeable progress has been reported in the ZnO aggregates-based DSCs that through enhanced light scattering via the controlled aggregation of ZnO nanocrystallites,^{13–16} a PCE of 6.1% has been achieved. However, ZnO aggregates-based DSC demonstrated much lower power conversion efficiency than the record efficiency of TiO₂ nanocrystalline DSC, in spite of the fact that ZnO has the similar electronic structure to and higher electron mobility than that of anatase TiO₂.¹⁷ Thus, the hierarchical structure of the TiO₂ film could be an ideal system for DSCs application. However, the photoelectrode film that was formed by TiO₂ aggregates synthesized with methods reported in literatures showed pretty poor conversion efficiency due to the non-ideal crystal structure and porosity.¹⁸ Such issues present many opportunities to further improve the photovoltaic performance of TiO₂ aggregates-based DSCs by developing TiO₂ aggregates with (1) proper facets and high surface area for dye adsorption and (2) providing suitable light scatters to improve light harvesting.

The following describes solar cells consisting of aggregated TiO₂ nanotubes, fabricated by the way of hydrothermal synthesis, and compares the overall light conversion efficiency to that of TiO₂ films fabricated from commercially-available nanoparticles (P25). Aspects to influence the operations of DSCs based on aggregated TiO₂ nanotubes have been systematically explored. By tailoring the morphology of aggregated TiO₂ nanotubes, a significantly enhanced PCE of 8.49% was achieved using the common N719 dyes without optimizing the device fabrication techniques. It is understood that such a high light conversion efficiency correlates with the larger surface area, the suitable facets and the presence of light scattering centers in our aggregated TiO₂ nanotubes photoelectrodes.

2. Experimental

2.1. *Synthesis and characterization of micron-sized aggregates of TiO₂ nanotubes*

Commercial grade, nanosize TiO₂ (Degussa Aeroxide P25), was a gift from Degussa Corp. (Parsippany, NJ) and used without any purification or treatment. The preparation was initiated by adding 1.0 g Dugussa Aeroxide P25 powder into a 40 mL aqueous solution of 10 M sodium hydroxide. After sonication for 30 min, this suspension was put into a Teflon-lined autoclave and heated to 150°C for 24 h. Then, the products were added into 60 mL hydrochloride (HCl) solutions (0.1 M) and stirred for 3 h. Subsequently, further treatment with HCl washing followed

by centrifuge at 3000 RPM. This acid washing was repeated for several times till the PH of the suspension reached at $\sim 3-5$. After that, the acid washing powder was subjected to ethanol washing in centrifuge tube with the ethanol of 20 mL. The final product was obtained by heating the resultant powder at 500°C for 2 h in air.

2.2. Solar cells testing and structural characterization

The preparation of the photovoltaic device and the testing were carried out according to the previously published protocols.¹³ Transmission electron microscopy (TEM) study was performed on a JEOL JSM-2010 microscope at 200 kV. X-ray diffraction (XRD) patterns were recorded on a Philips Xpert X-ray diffractometer using Cu K α radiation at $\lambda = 1.54 \text{ \AA}$. N₂ adsorption-desorption data were collected using a Quantachrome autosorb automated gas sorption system.

3. Results and Discussion

Shown in Fig. 1 are the SEM and TEM images of TiO₂ nanotubes powder heat treated at 500°C. It illustrates that the samples are made of 2–4 μm and oval

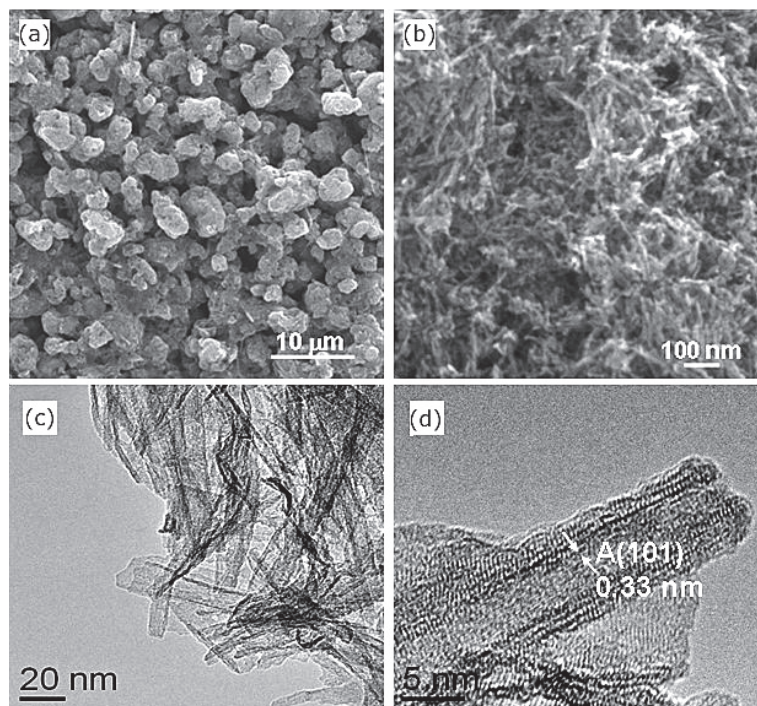


Fig. 1. SEM and TEM images of the TiO₂ nanotubes aggregates. (a) A low magnification SEM image of the aggregates; (b) a high magnification SEM image; (c) low magnification TEM images of sample after that treatment; (d) the high resolution TEM images of a single TiO₂ nanotube.

shaped aggregates which are densely packed [Fig. 1(a)]. In the high magnification SEM image, nanotube structure becomes plainly visible [Fig. 1(b)], showing no difference from the as prepared samples (not shown here), where the agglomeration of randomly orientated nanotube are observed. Apart from the SEM images, TEM was further used to examine the nanotube morphology retained in heat treated samples. As indicated in Fig. 1(c), it is seen that the diameter of TiO₂ nanotubes is in the range of ~10–20 nm, which provides a larger specific surface area for strong photons absorption and electron-hole generation and the resultant overall high light conversion efficiency. The preservation of the continuous nanotube structures is clearly evident in the high resolution TEM image [Fig. 1(d)], where it shows the high resolution TEM image of single nanotube from samples calcined at 500°C. Both the lattice planes perpendicular and parallel to nanotube axes are resolved, where the lattice constant corresponding to the (101) plane is about 0.33 nm, which is consistent with the commonly observed anatase lattice plane.

Figure 2 shows XRD patterns of TiO₂ nanotube powder of as-prepared and heat treated at 500°C, respectively. The nanotube diffraction pattern before calcination is indexed according to the H₂Ti₃O₇ structure (PDF# 036-0654), which is in accordance with the literature data.¹⁵ Samples annealed at 500°C possess pure anatase structure, where the indexed peaks are completely from the anatase phase (PDF# 002-0387) without any presence of rutile and brookite phase. For the same thickness TiO₂-based photoelectrode film, the photocurrent of the rutile-based DSCs is about 30% lower than that of the anatase-based cells, where the desirable anatase facets promote the dye absorption together with electron and holes generation, allowing for improving the solar cell performances.¹³

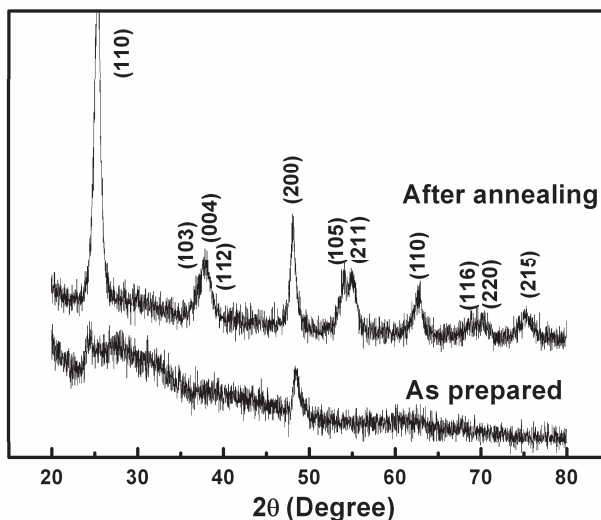


Fig. 2. XRD patterns of the as prepared nanotubes powder and nanotubes powder annealed.

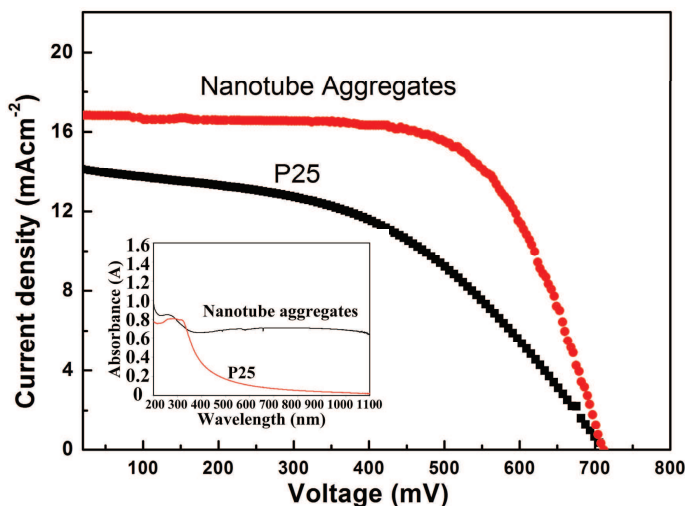


Fig. 3. The current–voltage curves of DSCs with photoelectrodes made of TiO₂ nanotube aggregates annealed at 500°C. The bottom left inset is absorption spectra of the photoelectrodes made of TiO₂ nanotube aggregates and P25 nanoparticles before dye loading.

Figure 3 shows the typical photovoltaic behavior of DSCs using TiO₂ nanotube aggregates as photoelectrode film while the cells were irradiated by AM 1.5 simulated sunlight with a power density of 100 mW/cm². The values of short-circuit current density (J_{sc}), open-circuit voltage (V_{oc}), fill factor (FF), are found to be 16.8 mA/cm², 710 mV and 66% respectively, yielding an overall power conversion efficiency (η) of 7.9%, much higher than that obtained for commercially-obtained P25, where short-circuit current density, open-circuit voltage, FF and the conversion efficiency were shown to be 14.1 mA/cm², 702 mV, 48.2% and 4.77% respectively.

The enhancement in short-circuit current density is the indication of the improvement in light absorption behavior associated with the presence of TiO₂ nanotube aggregated structure, resulting in higher photon absorption by way of light scattering. The TiO₂ nanotubes aggregates are very similar to those reported in ZnO,^{13–15} thus, may well serve as light scattering centers to enhance light harvesting. Therefore, in TiO₂ nanotubes aggregates based solar cell, TiO₂ nanotubes aggregates form light scattering centers, which may cause optical reflection and diffusion and therefore, significantly extend the distance that the light travels within the film. The light scattering properties of the aggregates are more revealed in the UV absorption spectrum (bottom left inset of Fig. 3). For a better comparative study, the absorption behavior experiment of commercially-obtained P25 was performed under identical processes. TiO₂ nanotubes aggregates possess the characteristic of typical intrinsic absorption below 390 nm and a continuous broad, besides, there is high background in the visible region due to the scattering effect of the micron-sized aggregates. In comparison, P25 only show the intrinsic absorption without much scattering in the large wavelength region.

In addition to the effect of light scattering, dye absorption is also thought to be another important issue that influences the light harvesting efficiency and the resultant conversion efficiency. In DSCs using TiO₂ as photoelectrode film, the conversion efficiency of TiO₂ nanotubes aggregates, as stated above, is significantly higher than that of 2.8% for TiO₂ nanocrystallites aggregates reported by Zhang *et al.*¹⁴ This had been partly attributed to the difference in facets for dye absorption. TiO₂ nanocrystallites aggregates contain anatase and a small fraction of brookite, while TiO₂ nanotube aggregates exhibit pure anatase phase without any fraction of rutile and brookite phase as shown in Fig. 2. Comparing with rutile and brookite phase, anatase TiO₂ has been proven to be favorable for both dye absorption and the injection efficiency of electrons transferring between dye and the photoelectrode.¹⁹ Therefore, the existence of suitable facets which contains TiO₂ nanotube aggregates would explain the higher conversion efficiency of 7.9%.

It is also worthy noting that the aggregates of TiO₂ nanotubes possess noticeably higher specific surface area, e.g., 424 m²/g for the sample before calcination, and ~147 m²/g when annealed at 500°C, resulting in ~50% improvement as compared with the conventional TiO₂ nanoparticles, typically < 90 m²/g, and the as-synthesized TiO₂ nanocrystallites aggregates grown by the hydrolysis process, where only 100 m²/g was attained.^{20,21} Such high specific surface area would be beneficial for more dye-loading, assuming other conditions are kept the same, and thus promoting higher power conversion efficiency.

4. Conclusion

It was found that using aggregates of TiO₂ nanotubes as photoelectrodes for DSCs demonstrated a promising higher power conversion efficiency for DSCs. The highest conversion efficiency of 7.9% and the largest short circuit density of 16.8 mA/cm² have been achieved. Such impressive photovoltaic performance is attributed to the presence of relatively high photo absorption surface area and the subsequent light scattering by the TiO₂ nanotubes aggregates, as well as the favorable facets for dye absorption. Further study is under the way and much higher power conversion efficiency is anticipated, providing the significant improvement of fabrication techniques attained for TiO₂ nanotubes aggregates as the DSCs photoelectrode.

Acknowledgments

The work was financially supported in part by the National Natural Science Foundation of China (Grant No. 11344010), the Fundamental Research Funds for the Central Universities (CQDXWL-2013-Z010). The work at the University of Washington was supported in part by the US Department of Energy (DE-FG02-07ER46467) and the Air Force Office of Scientific Research (AFOSR-MURI, FA9550-06-1-0326).

References

1. B. Ding *et al.*, *Adv. Energy Mater.* **1**, 415 (2011).
2. J. T. Xi *et al.*, *Nanosci. Nanotechnol. Lett.* **3**, 690 (2011).
3. M. Gratzel, *Nature* **414**(6861), 338 (2001).
4. B. Oregan and M. Gratzel, *Nature* **353**(6346), 737 (1991).
5. M. K. Nazeeruddin *et al.*, *J. Am. Chem. Soc.* **123**(8), 1613 (2001).
6. B. Ding *et al.*, *Adv. Energy Mater.* **1**, 415 (2011).
7. M. Adachi *et al.*, *J. Am. Chem. Soc.* **126**(45), 14943 (2004).
8. F. Labat *et al.*, *J. Am. Chem. Soc.* **131**(40), 14290 (2009).
9. X. Feng *et al.*, *Angewandte Chemie* **124**(11), 2781 (2012).
10. R. Stangl, J. Ferber and J. Luther, *Solar Energy Mater. Solar Cells* **54**(1–4), 255 (1998).
11. G. Rothenberger, P. Comte and M. Gratzel, *Solar Energy Mater. Solar Cells* **58**(3), 321 (1999).
12. S. Hore *et al.*, *Chem. Commun.* **15**, 2011 (2005).
13. T. P. Chou *et al.*, *Adv. Mater.* **19**(18), 2588 (2007).
14. Q. F. Zhang *et al.*, *Phys. Chemi. Chem. Phys.* **14**, 14982 (2012).
15. Q. F. Zhang *et al.*, *Angewandte Chemie-Int. Ed.* **47**(13), 2402 (2008).
16. Q. F. Zhang *et al.*, *Adv. Mater.* **21**, 4087 (2009).
17. Y. Xu and M. A. A. Schoonen, *Am. Mineral.* **85**, 543 (2000).
18. Q. F. Zhang *et al.*, *J. Nanophoton.* **4**, 041540 (2010).
19. N. G. Park, J. V. D. Lagemaat and A. J. Frank, *J. Phys. Chem. B* **104**(38), 8989 (2000).
20. Q. Chen *et al.*, *Acta Crystallographica Section B-Struct. Sci.* **58**, 587 (2002).
21. Z. R. R. Tian *et al.*, *J. Am. Chem. Soc.* **125**(41), 12384 (2003).